Aviation Electronics, Information Technology, Telecommunications, Electricals, and Controls (AVITEC)
Vol. 8, No. 1, February 2026, pp. 65-75, p-ISSN 2685-2381, e-ISSN 2715-2626
http://dx.doi.org/10.28989/avitec.v8i1.3544

Research Article

Ground Movement Tracking System for Airside Operations using Global Navigation Satellite System (GNSS) and Long Range (LoRa) Communication

Cokorda Dwija Wisnuardana[1]*, Johan Wahyudi[2], Muhammad Arif Sulaiman[3]
Air Navigation Engineering, Indonesian Civil Aviation Polytechnic, Indonesia

Article Info

Article history:
Submitted October 20, 2025
Accepted November 24, 2025
Published December 11, 2025

Keywords:
ground vehicle tracking;
airside operation;
aviation safety;
GNSS;
LoRa.

ABSTRACT

Accurate monitoring of ground vehicle and aircraft movement in the airport airside is essential to reduce the risk of incidents caused by limited coordination between controllers, pilots, and ground operators. This study proposes the design of a ground movement tracking system for airside operations, utilizing a Global Navigation Satellite System (GNSS) module (Matek M10Q-5883) and a Long Range (LoRa) communication module (LILYGO ESP32), integrated with a web dashboard for real-time visualization. The system was developed using the Waterfall methodology, covering requirement analysis, system design, hardware and software implementation, and performance testing in simulated airside conditions. Experimental results show that the system achieved an average coordinate deviation of only 0.000017º equivalent to about 1.7 meters compared to a reference device, and maintained reliable data transmission up to 1.4 km under line-of-sight conditions. These findings demonstrate that the proposed system provides accurate and stable monitoring of ground movements, offering a cost-efficient and weather-independent alternative to GSM-based solutions. In addition, by optimizing LoRa parameters, the system successfully extended its communication range beyond the ~1 km typically reported in related studies, highlighting its novelty and contribution to enhanced safety in airport operations.

Corresponding Author:
Cokorda Dwija Wisnuardana,
Air Navigation Engineering, Indonesian Civil Aviation Polytechnic, Tangerang, Indonesia,
Email: *cokvisnuardana@gmail.com

1. INTRODUCTION

Airside operations in airports involve the coordinated movement of aircraft and ground service vehicles, which must be monitored effectively to ensure safety and efficiency. Limited coordination among controllers, pilots, and ground vehicle operators can result in runway incursions and hazardous incidents, as highlighted in airside surveillance studies [1]. To address these challenges, digital and IoT-based monitoring systems have increasingly been proposed for airport environments, particularly those leveraging wireless sensor networks and long-range communication protocols [2]. In practical terms, the proposed system provides airport managers with real-time visibility of ground vehicle movement, enabling faster decision-making, reducing the likelihood of runway incursions, and supporting more efficient allocation of ground support resources

Traditional GPS-based monitoring has often relied on GSM networks, as in the web-based vehicle tracking system by Rahman et al. (2019) [3]. However, GSM coverage can be inconsistent in complex environments, limiting reliability. Asmar et al. (2024) [4] demonstrated that combining GPS with LoRa in transportation monitoring improves stability, though their work focused on palm oil transport and employed the Neo-6M GPS module, which has known limitations in accuracy and update rates. Yoshua et al. (2020) [5] further explored multi-node LoRa communication using a master–slave configuration, proving its feasibility for distributed IoT applications.

The advancement of GNSS modules has enhanced positioning accuracy. Akbar et al. (2024) [6] highlighted the improved performance of the Ublox M10Q-5883 compared to older Neo-6M devices, while Kim & Nam (2024) [7] presented an integrated LoRa and dual-band GNSS antenna achieving compact and efficient

designs. Low-cost GNSS–LoRa trackers have also been developed for wildlife monitoring [8] and broader IoT localization [9], indicating their adaptability to different mobility scenarios.

The role of LoRa in airport digitalization has also been recognized. Semtech's deployment in smart airport projects illustrates LoRa's feasibility for large-area IoT connectivity [10]. Tang et al. (2025) [11] measured LoRa propagation using aerial and ground gateways in urban areas, showing the influence of environment and line-of-sight conditions. Aernouts & Janssen (2021) [12] compared LoRa localization methods with and without GNSS, revealing trade-offs in accuracy and scalability. Wang et al. (2020) [13] explored GNSS-based scheduling of airport ground support equipment, further proving the value of precise and reliable tracking in airside operations.

Performance analyses of LoRa in aviation and IoT contexts confirm its potential. Jalalizad & Khorsandi (2024) [14] examined LoRa-based on Air to Ground communication, identifying limitations under N-LOS conditions. Osman & Abbas (2022) [15] benchmarked LoRa against Sigfox, showing LoRa's superior reliability in IoT deployments. Alipio et al. (2024) [16] reviewed testing methodologies for LoRa performance, while Juledi et al. (2024) [17] and Irianto (2022) [18] validated LoRa's application in vehicular and irrigation monitoring. Janssen et al. (2023) [19] conducted a comprehensive survey on IoT positioning techniques that combine LPWAN, GNSS, and emerging LEO satellite constellations, this reinforces the importance of hybrid approaches, including LoRa–GNSS integration, for developing reliable and energy-efficient tracking solutions in large-scale operational environments. Enriko (2023) [20] studied LoRa gateway coverage and capacity, providing insights into large-scale deployment strategies.

Despite these advancements, existing studies still present limitations that restrict their applicability to airside operational requirements. Rahman et al.[3] relied on GSM-based transmission, which introduces latency, dependence on cellular network quality, and unstable update intervals, making it unsuitable for controlled airport environments where communication reliability is critical. Likewise, Asmar et al.[4] employed the single-band Neo-6M GPS module, whose limited satellite reception results in lower positioning accuracy and slower update rates compared to modern multi-band GNSS receivers. Meanwhile, although Handoko et al.[21] used the newer M10 GNSS module, their implementation with the SX1278 LoRa transceiver achieved a maximum range of only 500 meters, which is insufficient for wide-area airside coverage. These limitations collectively highlight the unresolved need for a tracking system that simultaneously offers higher GNSS accuracy, faster and more stable update rates, and extended LoRa communication range tailored specifically for airside vehicle operations.

This study addresses these gaps by developing and validating a GNSS–LoRa ground-movement tracking system specifically designed for airside operations, with the objective of improving positioning accuracy through a multi-band M10-based GNSS solution and extending LoRa communication range beyond the limitations of previous works; the system further contributes by providing a real-time, low-latency monitoring platform that supports operational situational awareness and enhances the safety and efficiency of airport ground movements.

2. RESEARCH METHODS

2.1 Research Flow

The research was conducted following the Waterfall model as shown in Figure 1, which consists of five sequential stages: requirement analysis, system design, implementation, testing, and maintenance [22]. In the requirement analysis stage, system requirements were identified through a review of related works and the operational needs of airport airside environments. The design stage involved preparing wiring diagrams, hardware schematics, and database structures for the server. During the implementation stage, the hardware was assembled and programmed, while the web dashboard was developed for real-time visualization. Testing was carried out through static and dynamic experiments to evaluate GNSS accuracy and LoRa communication performance under both line-of-sight (LOS) and non-line-of-sight (NLOS) conditions. Finally, the maintenance stage focused on evaluating and refining system parameters based on testing outcomes [23].

The hardware configuration included the Matek GNSS M10Q-5883 receiver (multi-constellation GNSS with integrated compass), the TTGO T-Beam ESP32 LoRa development board with an 868/915 MHz LoRa transceiver, a 3.7 V, 2200 mAh lithium battery, and a laptop/PC server. A Wi-Fi modem was employed to support connectivity for the web dashboard.

The software environment comprised the Arduino IDE 1.8.19 for microcontroller programming [24] and multiple firmware libraries: TinyGPS++ v1.0.3 for GNSS data parsing, LoRa by Sandeep Mistry v0.8.0 for LoRa communication, AXP202X v1.1.0 for power management, Adafruit SSD1306 v2.5.7 for OLED display control, and Adafruit GFX v1.11.9 On the server side, MySQL Server 8.0 was used for data storage management [25], and Visual Studio Code v1.84 with the OpenStreetMap API was employed for developing the web-based dashboard interface [26].

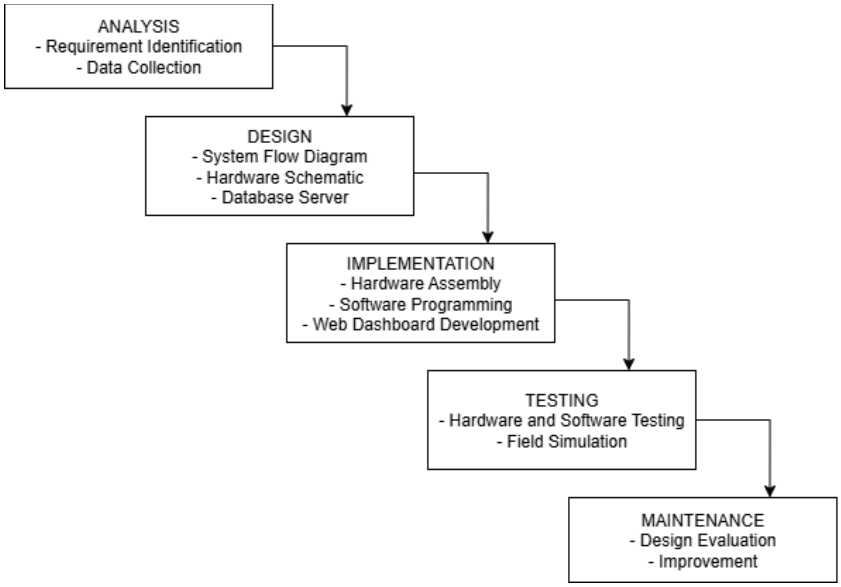

Figure 1. Waterfall method diagram

2.2 Overview of The System

The prototype consisted of two subsystems: (i) a transmitter installed on ground vehicles operating in the airside environment, and (ii) a receiver connected to a server for data storage and visualization, as shown in Figure 2. The transmitter collected GNSS data and transmitted it via LoRa, while the receiver parsed the incoming packets and stored them in a MySQL database, enabling real-time visualization on the web dashboard.

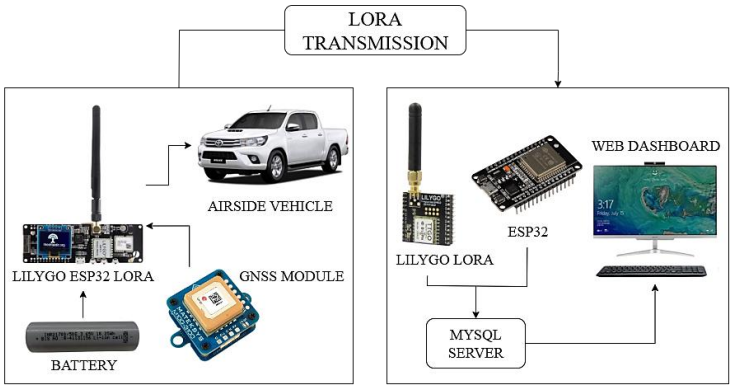

Figure 2. System overview

2.3 System Design

2.3.1 Transmitter Design

The transmitter was built on a LILYGO TTGO T-Beam ESP32 LoRa board integrated with the Matek M10Q-5883 GNSS module and is powered by an external battery. The wiring configuration is presented in Table 1, and the transmitter connection diagram is shown in Figure 3. The Arduino sketch reads GNSS NMEA sentences at a sampling rate of 1 Hz, parses them using TinyGPS++, and transmits packets via LoRa. Each LoRa packet contained a structured payload:

<ID_Device, Latitude, Longitude, Altitude, Timestamp>

LoRa parameters were set to default values: frequency 868 MHz, +14 dBm transmit power, spreading factor SF7, 250 kHz signal bandwidth, and coding rate 4/5. The timestamps were synchronized using GNSS time (UTC) provided by the M10Q module, ensuring consistency across devices.

Table 1. Transmitter Pinout Interface

Pin LILYGO		Pin Matek GNSS	Information
GND	⇔	G	Ground Pinout
-	⇔	DA	-
-	⇔	CL	-
GPIO 13	⇔	TX	Transmitter Pinout
GPIO 33	⇔	RX	Receiver Pinout
5V	⇔	5V	+5V Power Source Pinout

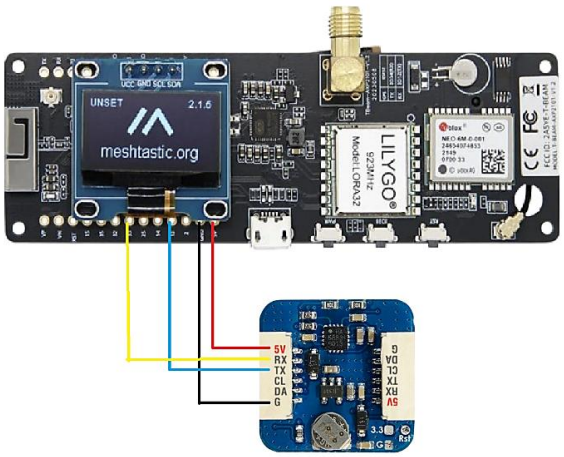

Figure 3. Transmitter Connection Diagram

2.3.2 Receiver Design

The receiver used a ESP32 and TTGO LoRa module configured to listen on the same frequency (868 MHz), spreading factor SF7, bandwidth 250 kHz, and coding rate 4/5. Received packets were parsed and forwarded via serial to a Python script on the server, which inserted data into a MySQL table with fields: id_device, latitude, longitude, altitude, speed, and timestamp. The wiring interface is shown in Table 2, and the receiver connection diagram is shown in Figure 4.

Table 2. Receiver Pinout Interface

Pin ESP32		Pin LoRa	Information
3V3	⇔	3V3	+3V Power Input
GND	⇔	GND	Ground Pinout
D19	⇔	MISO	SPI Data Out
D18	⇔	SS	Chip Select (Activing LoRa)
D5	⇔	SCK	SPI Clock Pinout
D23	⇔	IO0	Interrupt Pinout

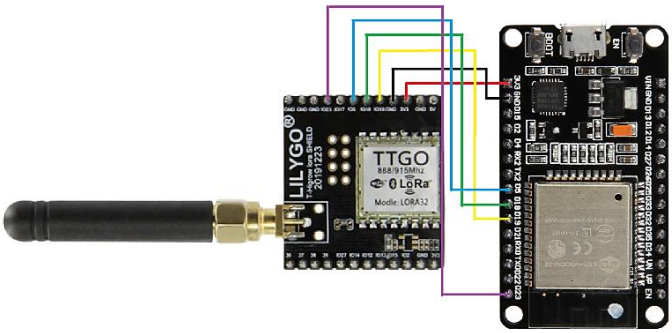

Figure 4. Receiver connection diagram

2.3.3 Database Server

A MySQL database was created to store GNSS data received by the system. The database structure defines fields such as ID, timestamp, latitude, and longitude, functioning as the central repository for the dashboard application. The table stucture made on the MySQL server is shown in Table 3.

Table 3. Table structure format

Column Name	Data Type	NN	PK	Extra
Id	INT	✓	✓	Auto Increment
Device_id	VARCHAR	✓		
Latitude	Double	✓		
Longitude	Double	✓		
Altitude	Double			
Speed	Double			
timestamp	Datetime			Default: Current_Timestamp

2.3.4 Web Dashboard

The visualization dashboard was implemented with HTML, PHP, and JavaScript, utilizing Leaflet.js for geospatial rendering. Unlike periodic refresh mechanisms, the system adopted PHP Server-Sent Events (PHP_SSE), allowing markers on the map to be updated automatically each time new data were inserted into the database, thus ensuring real-time accuracy without unnecessary refresh cycles.

2.4 Calibration and Validation

Prior to testing, the GNSS module was calibrated through a cold start procedure in an open outdoor area to maximize satellite acquisition. A sufficient waiting time ensured the module achieved a fixed position with optimal accuracy. Measurements were then validated against a reference device by Garmin GPSMap 62s. LoRa performance was evaluated under line-of-sight (LOS) and non-line-of-sight (NLOS) conditions to assess coverage and signal stability.

2.5 Data Sampling

GNSS data were sampled and transmitted at a fixed frequency of 1 Hz. This sampling rate is determined by the transmitter firmware, in which the GPS parsing routine (smartDelay(1000)) and LoRa transmission interval (delay(1000)). The database was configured with a rolling buffer that stores a maximum of 250 most recent samples. When the limit is reached, older records are automatically deleted to maintain consistent memory usage. As a result, each test session yields up to 250 valid GNSS–LoRa samples, corresponding to approximately 15 minutes of continuous data acquisition. This configuration ensures stable throughput for both accuracy evaluation and communication range testing while maintaining reproducibility and consistent sample size.

LoRa data transmission sampling were performed under two environmental conditions: open Line-of-Sight (LOS) and partially obstructed Non-Line-of-Sight (NLOS) scenarios within the airside perimeter. Each test consisted of more than 10 transmission attempts per distance point to ensure statistical consistency.

2.6 Testing Methods

2.6.1 GNSS Accuracy Test

The accuracy of the Matek GNSS M10Q-5883 module was evaluated using two complementary testing approaches: static testing and dynamic trajectory testing. Both methods compared the coordinate readings of the prototype device with two reference receivers, with those of a Garmin GPSMAP 62s and a smartphone-based GNSS, to assess positional stability and real-world tracking performance.

In the static testing method, the prototype was placed at several fixed points within the Indonesian Aviation Polytechnic Curug campus. At each point, both latitude and longitude readings were sampled simultaneously from all devices. Accuracy was quantified by computing the geodesic distance between coordinate pairs from the prototype and the reference devices using the Haversine formula, which accounts for Earth's curvature. The Haversine equation is expressed as Equation (1).

$$d = 2R \cdot \arcsin\left(\sqrt{\sin^2\left(\frac{\Delta\varphi}{2}\right) + \cos(\varphi_1)\cos(\varphi_2)\sin^2\left(\frac{\Delta\lambda}{2}\right)}\right) \quad (1)$$

description: d : geodesic distance between two coordinate points (meters)
R : Earth's radius (6,371,000 meters)
φ_1, φ_2 : latitudes of point 1 and point 2 (radians)
λ_1, λ_2 : longitudes of point 1 and point 2 (radians)
$\Delta\varphi = \varphi_2 - \varphi_1$: difference in latitude (radians)
$\Delta\lambda = \lambda_2 - \lambda_1$: difference in longitude (radians)

For the dynamic testing method, the GNSS module, Garmin GPSMAP 62s, and smartphone were carried simultaneously along a predefined route to evaluate real-time tracking performance. Each device recorded its coordinate stream while moving, enabling trajectory comparison through polyline analysis on the web dashboard. This test assessed the prototype's ability to capture movement changes, maintain satellite lock, and follow the true path under varying environmental conditions such as partial obstruction, turns, and motion-induced multipath effects.

2.6.2 LoRa Range Test

The LoRa communication performance was evaluated under two environmental conditions: Line-of-Sight (LOS) and Non-Line-of-Sight (N-LOS). The LOS test was conducted along an unobstructed straight route to assess ideal propagation, whereas the N-LOS test introduced partial obstructions such as buildings, vehicles, and vegetation to represent realistic airside conditions. In both scenarios, the transmitter was mounted on a moving vehicle while the receiver remained stationary, and packet reception, RSSI, and SNR were recorded at incremental distances.

Parameter optimization was performed to improve link performance beyond the default configuration (SF7, 250 kHz bandwidth, CR 4/5, +14 dBm). Several trials were conducted by increasing the spreading factor, narrowing bandwidth, and raising transmission power. Based on technical specifications the SX1276 module

supports up to +20 dBm output. All LoRa transmissions were configured to operate at 923 MHz, which complies with the Indonesian ISM band allocation under the AS923 LoRaWAN Regional Parameters [27]. The allowed maximum EIRP for this band is 30 dBm, ensuring that the selected configuration remained within regulatory limits. This frequency selection also avoids interference with licensed aviation communication bands, making it suitable for integration within airport operational environments.

3. RESULTS AND DISCUSSION

3.1 GPS Accuracy Test Result

The first was a static method, which collected samples of longitude and latitude coordinates at several fixed points. As an example, the coordinate deviation can be calculated with Haversine Formula from the first data sample, which was obtained at a fixed location in Barak Delta, by comparing the readings of the prototype GPS (−6.285450, 106.565800) with those of the smartphone GPS (−6.285448, 106.565815) as follows, and the comparative results are presented in Table 4 showing deviations between the three devices.

Data: Point 1 (Prototrype GPS) : lat1 = -6.285450, lon1 = 106.56580
Point 2 (Reference GPS) : lat2 = -6.285448, lon2 = 106.565815

- Convert degrees to radians:
  $\varphi_1 = -0.109708592$ rad
  $\varphi_2 = -0.109708557$ rad
  $\Delta\varphi = 3.4906585 \times 10^{-8}$ rad
  $\Delta\lambda = 2.61799388 \times 10^{-7}$ rad
- Haversine equation:
  $d = 2R \cdot \arcsin\left(\sqrt{\sin^2(\frac{\Delta\varphi}{2}) + \cos(\varphi_1)\cos(\varphi_2)\sin^2(\frac{\Delta\lambda}{2})}\right)$
  $d = 1.67$ meters

Table 4. Comparison of coordinate differences between devices

Device	Coordinate		Difference Between Prototype GPS & Garmin	Difference Between Prototype GPS & Smartphone
	Latitude	Longitude		
Barak Delta				
Prototype GPS	-6.28545	106.56580	0.000000º (0 meters)	0.000015º (1.67 meters)
Garmin	-6.28545	106.56580		
Smartphone	-6.285448	106.565815		
Lab CNS				
Prototype GPS	-6.28552	106.56976	0.000014º (1.55 meters)	0.000019º (2.11 meters)
Garmin	-6.28551	106.56975		
Smartphone	-6.285526	106.569741		
Teknik Penerbangan Building				
Prototype GPS	-6.28262	106.57122	0.000014º (1.55 meters)	0.000018º (2 meters)
Garmin	-6.28263	106.57121		
Smartphone	-6.282611	106.571236		
Pura PPIC				
Prototype GPS	-6.28610	106.56803	0.000000º (0 meters)	0.000013º (1.44 meters)
Garmin	-6.28610	106.56803		
Smartphone	-6.286111	106.568038		
Aviamart				
Prototype GPS	-6.28631	106.56437	0.000020º (2.22 meters)	0.000021º (2.33 meters)
Garmin	-6.28631	106.56435		
Smartphone	-6.286319	106.564351		
Average difference between GPS Tools & Garmin			0.000009º (1 meters)	
Average difference between GPS Tools & Smartphone			0.000017º (1.89 meters)	

Based on these results, the average deviation between the prototype and the Garmin GPS was 0.000009º, with the smallest difference of 0.000000º and the largest of 0.000020º. When compared with the smartphone GPS, the average deviation was 0.000017º, equivalent to about 1.7 meters, with the smallest of 0.000013º and the largest of 0.000021º. These relatively small deviations indicate that the prototype system is capable of displaying accurate coordinate points of the monitored object.

The Matek GNSS M10Q-5883 demonstrated high positional stability under both static and dynamic testing conditions. Using the Haversine equation (as described in Section 2.6), the geodesic distance between the prototype and the reference coordinates showed an average static error of 1.67 m, which is consistent with the expected accuracy range for L1 multi-GNSS receivers in open-sky conditions. This result represents a significant improvement compared to Rahman et al. [3], whose system—based on the Neo-6M and GSM communication—achieved position errors of 2.4–2.5 m under similar open-sky conditions. The improvement of approximately 31–34% is largely attributable to the M10Q module's ability to track more satellite constellations simultaneously, improving dilution of precision (DOP) and allowing faster position fixes and shorter update intervals of 1–3 seconds through LoRa transmission. This improvement is attributed to the higher sensitivity, dual-frequency correction capability, and faster TTFF (Time to First Fix) of the M10Q module.

The second method was a dynamic test, which evaluated the trajectory recorded by each device. A predefined route was traversed while carrying the three devices simultaneously. Each device recorded the object's movement history and visualized it as a polyline on its respective map display. The recorded tracks are illustrated in the Figure 5.

Figure 5. Tracking line comparasion

The results showed that the polyline traces from the Matek GNSS module closely matched those from the Garmin and smartphone devices, indicating reliable dynamic tracking performance. The trajectory recorded by the prototype followed the reference polylines closely, maintaining continuous satellite lock even during turns or brief partial obstructions. This performance contrasts with Asmar et al.[4], whose Neo-6M–LoRa implementation exhibited frequent coordinate jumps during vehicle motion, primarily due to the Neo-6M's slower update rate and weaker multipath rejection. The consistency of the dynamic path in this study indicates improved robustness in motion-induced multipath conditions, as well as better filtering of short-term noise. Comparing with Handoko et al.[21], who also used the M10 series but for wearable tracking, this study demonstrates similar stability yet by used for airside vehicle.

Mechanistically, the superior accuracy can be explained by several factors. First, reduced multipath effects and improved satellite visibility under open-sky conditions in the airside environment minimized coordinate deviation. Second, the multi-band design of the Matek M10Q module provides the ability to mitigate ionospheric and tropospheric delays by using two carrier frequencies, which significantly improves positional stability compared with single-band GNSS receivers such as the Neo-6M used in earlier research. Third, the use of an active ceramic antenna enhances signal-to-noise ratio, allowing the receiver to maintain more consistent satellite locks. Minor deviations observed during dynamic testing are likely caused by short-term loss of satellite lock during rapid heading changes or reflections from metallic surfaces around service roads—conditions typical of airport airside environments.

3.2 LoRa Range Test Result

The transmission range of the LoRa module was tested in two environmental conditions: Non-Line of Sight (N-LOS) and Line of Sight (LOS). The Received Signal Strength Indicator (RSSI) was measured to assess radio signal strength at various distances.

N-LOS Testing**.** In obstructed environments, the default LoRa configuration at 50 meters yielded a strong RSSI of –65 dBm. Reliable communication was maintained up to 600 meters, where the RSSI was –96 dBm. Beyond 600 meters, at an RSSI of –98 dBm, the link became unstable and data transmission failed. The results are summarized in the Table 5.

Table 5. LoRa N-LOS area test results

Distance	RSSI	Status
50 m	-65 dBm	Data Valid
100 m	-70 dBm	Data Valid
200 m	-80 dBm	Data Valid
300 m	-87 dBm	Data Valid
400 m	-90 dBm	Data Valid
500 m	-93 dBm	Data Valid
600 m	-96 dBm	Data Valid
> 600 m	-	Data Crash, Occurred at RSSI: -98 dBm

LOS Testing**.** In open-field conditions, LoRa showed superior performance. At 50 meters, the RSSI was –55 dBm, and stable communication continued up to 1000 meters with an RSSI of –100 dBm. At distances beyond 1000 meters, the link was lost at –101 dBm. Data transmission remained stable with update intervals of 1–2 seconds. The results are shown in the Table 6.

Table 6. LoRa LOS area test results

Distance	RSSI	Status
50 m	-55 dBm	Data Valid
100 m	-64 dBm	Data Valid
200 m	-68 dBm	Data Valid
300 m	-71 dBm	Data Valid
400 m	-76 dBm	Data Valid
500 m	-82 dBm	Data Valid
600 m	-87 dBm	Data Valid
700 m	-90 dBm	Data Valid
800 m	-94 dBm	Data Valid
900 m	-97 dBm	Data Valid
1000 m	-100 dBm	Data Valid
>1000 m	-	Data Crash, Occurred at RSSI: -101 dBm

Parameter Optimization**.** To maximize transmission range and sensitivity of LoRa, while maintaining stability. Parameter tuning was applied to both the transmitter and receiver, adjusting transmitter power, spreading factor, signal bandwidth, and coding rate. Although the SX1276 chipset supports a maximum output of +20 dBm, preliminary thermal stress observations showed that continuous operation at maximum power caused excessive heating and increased the risk of RF front-end component degradation. Therefore, +18 dBm was selected as an optimal operating point, providing improved communication range in wide airside environments while ensuring thermal stability and minimizing long-term hardware degradation risk. The optimization process is summarized in the Table 7.

Table 7. LoRa parameter optimization

Parameter	Before Optimization (Default)	After Optimization
Power Transmitter	+14 dBm	+18 dBm
Spreading Factor	SF7	SF10
Signal Bandwidth	250 kHz	125 kHz
Coding Rate	4/5	4/7

Post-Optimization Testing**.** After parameter adjustments, LoRa communication reached up to 1400 meters with an RSSI of –103 dBm and an update rate of 1–3 seconds. The results after optimization are presented in the Table 8.

These findings indicate that LoRa, when optimally configured, can extend its effective transmission range by approximately 40% compared to the default configuration. The prototype system was able to transmit real-time coordinate data reliably within 1.4 km under LOS conditions, while still maintaining acceptable performance in N-LOS scenarios. When compared to prior studies, the proposed system outperforms several related implementations. Asmar et al.[4] achieved a maximum distance of 850 meters under similar LOS conditions using the E220 LoRa module, meaning the current study achieved a 64% longer range. while Handoko et al.[21], who used the same M10 GNSS module but an SX1278 LoRa transceiver, reported a communication range of only 500 meters. The SX1276 used in this study has superior receiver sensitivity, which explains the substantial range difference. Similarly, Lin et al.[28] using the SX1276 LoRa module achieved 1 km transmission distance under similar conditions without LoRa parameter optimalization, which is slightly below the optimized performance in this study. The additional 400 m gain in our prototype can be attributed to refined antenna

alignment, higher transmit power, and optimized spreading factor. Hence, this research demonstrates an improved LoRa range performance and overall system precision.

Table 8. LoRa Range Test After Optimalization

Distance	RSSI	Status
50 m	-36 dBm	Data Valid
100 m	-41 dBm	Data Valid
200 m	-52 dBm	Data Valid
300 m	-58 dBm	Data Valid
400 m	-67 dBm	Data Valid
500 m	-72 dBm	Data Valid
600 m	-75 dBm	Data Valid
700 m	-79 dBm	Data Valid
800 m	-84 dBm	Data Valid
900 m	-88 dBm	Data Valid
1000 m	-91 dBm	Data Valid
1100 m	-93 dBm	Data Valid
1200 m	-96 dBm	Data Valid
1300 m	-99 dBm	Data Valid
1400 m	-101 dBm	Data Valid
>1400 m	-	Data Crash, Occurred at RSSI: -103 dBm

Mechanistically, the improved transmission range can be attributed to several physical and configuration factors. The antenna placement and orientation directly influence the radiation pattern and minimize signal obstruction or ground reflection losses. Higher transmission power (Tx Power) increases the effective radiated energy, thereby extending the maximum detectable range. However, it also raises power consumption, so a balance is required between range and energy efficiency. The Spreading Factor (SF) determines the number of chirps used to encode each symbol, increasing SF improves receiver sensitivity by allowing better signal demodulation under weak-signal conditions, but also lowers data rate and increases latency. Meanwhile, the Coding Rate (CR) introduces forward error correction bits, a higher CR improves robustness against noise and interference, enabling longer communication distance, but reduces effective throughput. Thus, the optimal configuration represents a trade-off between communication stability and data transmission efficiency.

3.3 Overall System Performance

Overall, the integration of the GNSS M10Q-5883 with the LoRa SX1276 module provides a stable, energy-efficient, and highly accurate ground tracking system suitable for airport airside applications. The system successfully transmits coordinate data in real time to the server and visualizes it on the web dashboard. Compared with previously published systems (as shown in Table 9), this implementation achieves 30–40% greater transmission distance and 30% higher positional accuracy. The accuracy results obtained in this study also demonstrate operational relevance when benchmarked against international standards. According to the ICAO A-SMGCS Manual (Doc 9830)[29], the recommended surveillance accuracy for surface movement monitoring is approximately 6 meters to support safe and effective ground movement monitoring. The static test deviation achieved by the proposed Matek M10-based system—approximately 1.6–1.7 meters—is therefore well within ICAO's recommended accuracy envelope. This alignment with ICAO guidance reinforces the feasibility of the proposed GNSS–LoRa tracking prototype for practical airside operations, particularly in applications involving vehicle tracking, routing supervision, or operational safety enhancement. These results demonstrate that the combination of GNSS and LoRa technologies offers a reliable foundation for low-power, long-range monitoring systems in complex operational environments such as airport airside areas.

Table 9. Comparison of GNSS and LoRa Performance with Related Studies

Study / Author	GNSS Module	Communication Type	Max Range (m)	Avg. Accuracy (m)	Data Interval (s)	Remarks
Abdul Chalel (2019) [22]	u-blox NEO-6M (Single Band)	GSM / GPRS	–	2.4 – 2.5	~10	Dependent on cellular signal; high latency.
Asmar Ramadhan et al. (2024) [4]	NEO-6M	LoRa E220	850	2.5	5	Limited range; signal loss beyond 850 m.
Tri Handoko et al. (2024) [21]	M10 (Multi-Band)	LoRa SX1278	500	1.9	2–3	Stable short-range link; limited LoRa output power.
Shangwei Lin et al. (2024) [28]	MAX-7Q	LoRa SX1276	1000	10.0	2–3	Good LOS performance; low GNSS precision.
This Study (2025)	Matek M10Q-5883 (Multi-Band)	LoRa SX1276	**1400**	**1.7**	**1–3**	Improved GNSS accuracy and extended range after LoRa parameter optimization.

4. CONCLUSION

The findings of this study confirm that the initial hypotheses were supported: the use of the Matek GNSS M10Q-5883 significantly improved positioning accuracy compared with earlier Neo-6M–based systems, and the optimized LoRa configuration successfully extended communication range for airside ground-movement tracking. Static accuracy tests achieved a geodesic error of 1.67 m, representing an improvement of over 30% relative to comparable GSM-Neo-6M implementations, while dynamic tests demonstrated stable trajectory tracking under operational motion. Likewise, the LoRa link achieved a maximum LOS range of 1.4 km after parameter optimization, exceeding previous SX1278 and E220-based studies. Despite these positive outcomes, the system remains constrained by limited test-area size, reduced performance in dense N-LOS conditions, and operation with a single mobile node. Future work should expand testing to multi-node deployments across a wider airport sector to further validate scalability and operational readiness.

ACKNOWLEDGMENTS

The authors would like to express their sincere gratitude to Politeknik Penerbangan Indonesia Curug and the Air Navigation Engineering Study Program for their continuous support, facilities, and guidance throughout the completion of this research. Special appreciation is also extended to Course TELNAV 29, whose encouragement and collaboration have been an invaluable source of motivation and pride during this work.

REFERENCE

[1] P. Thai, S. Alam, N. Lilith, P. N. Tran, and B. N. Thanh, "Deep4Air: A Novel Deep Learning Framework for Airport Airside Surveillance," *Proc. IEEE Int. Conf. Multimedia Expo Workshops* (*ICMEW*), Oct. 2020. https://doi.org/10.1109/ICMEW53276.2021.9456005.

[2] E. S. Hasibuan, A. Panjaitan, and R. P. Simanjuntak, "Utilization of Multihop Communication Technology Based on LoRa for Maintenance of Airport Street Lighting," *International Journal of Health Engineering and Technology*, vol. 4, no. 3, Sep. 2025.

[3] A. C. Rahman, W. A. Arimbawa, and A. H. Jatmika, "Implementation of Internet of Things on Web-Based Motor Vehicle Tracking Information System Using GPS," *JTIKA*, vol. 1, no. 1, 2019. https://doi.org/10.29303/jtika.v1i1.10.

[4] R. H. Asmar, A. Yuwaldi, and H. Fahri, "Prototype of IoT System for Tracking Dump Trucks Transporting Palm Oil Fruit Based on GPS and LoRa Modules," *KITEKTRO*, vol. 9, no. 3, 2024. https://doi.org/10.24815/kitektro.v9i3.41250.

[5] A. Yoshua, R. Primananda, and A. S. Budi, "Implementing Multi-Node Sensor Data Transmission Using the Master-Slave Method in LoRa Communication," *Jurnal Pengembangan Teknologi Informasi dan Ilmu Komputer*, vol. 4, no. 10, pp. 3445–3454, 2020. [Online]. Available: https://j-ptiik.ub.ac.id/index.php/j-ptiik/article/view/7993

[6] S. A. Akbar, C. Putra, D. Liya, and Y. Sabila, "Implementation of Portable Antenna Design based on Ublox M10Q-5883 for Unmanned Aerial Vehicle Movement Tracking," *TRANSIENT: Jurnal Ilmiah Teknik Elektro*, vol. 13, no. 4, 2024.

[7] S. Kim and S. Nam, "Implementation of an Integrated LoRa and Dual-Band GNSS Antenna in a Compact Package," *Journal of Electromagnetic Engineering and Science*, vol. 24, no. 6, pp. 632–640, Nov. 2024. https://doi.org/10.26866/jees.2024.6.r.269.

[8] A. F. Parlin, N. A. Horning, J. P. Alstad, B. J. Cosentino, and J. P. Gibbs, "Low-cost, LoRa GNSS Tracker for Wildlife Monitoring," *HardwareX*, vol. 23, Sep. 2025. https://doi.org/10.1016/j.ohx.2025.e00669.

[9] H. Ruan, P. Sun, Y. Dong, H. Tahaei, and Z. Fang, "An Overview of LoRa Localization Technologies," *Computers, Materials and Continua*, vol. 82, no. 2, pp. 1645–1680, 2025. https://doi.org/10.32604/cmc.2024.059746.

[10] J. P. Tomás, "Semtech Deploys LoRa Technology for Smart Airport Project in Turkey," *RCR Wireless News*, Jun. 21, 2019.

[11] W. Tang et al., "Measurement of LoRa signal propagation in urban areas utilizing aerial gateway and ground gateway," *Scientific Data*, vol. 12, no. 1, p. 1464, 2025. https://doi.org/10.1038/s41597-025-05802-2.

[12] M. Aernouts, T. Janssen, R. Berkvens, and M. Weyn, "LoRa Localization: With GNSS or Without?," *IEEE Internet of Things Magazine*, vol. 5, no. 3, pp. 152–157, 2022. https://doi.org/10.1109/IOTM.001.2200019.

[13] S. Wang, Y. Che, H. Zhao, and A. Lim, "Accurate Tracking, Collision Detection, and Optimal Scheduling of Airport Ground Support Equipment," *IEEE Internet of Things Journal*, vol. 8, no. 1, pp. 572–584, 2021. https://doi.org/10.1109/JIOT.2020.3004874.

[14] S. Jalalizad and K. Khorsandi, "Performance Evaluation of LoRa Networks for Air-to-Ground Communications," M.S. thesis, KTH Royal Institute of Technology, Stockholm, Sweden, 2023.

[15] N. Izzeldin and E. B. Abbas, "Performance Evaluation of LoRa and Sigfox LPWAN Technologies for IoT," *Academic Journal of Research and Scientific Publishing*, vol. 4, 2022.

[16] M. Alipio and M. Bures, "Current testing and performance evaluation methodologies of LoRa and LoRaWAN in IoT applications: Classification, issues, and future directives," *Internet of Things*, vol. 25, p. 101053, 2024. https://doi.org/10.1016/j.iot.2023.101053.

[17] A. P. Juledi, M. K. Huda, M. T. D. Putra, L. D. Samsumar, P. D. P. Adi, and Y. Nurdiansyah, "Performance Evaluation of LoRa 923 MHz for the Internet of Things," in *2024 IEEE 10th Information Technology International Seminar* (*ITIS*), Bandung, Indonesia, 2024, pp. 30–34. https://doi.org/10.1109/ITIS57492.2024.10845693

[18] K. D. Irianto, "Performance Evaluation of LoRa in Farm Irrigation System with Internet of Things," *Kinetik*, vol. 7, no. 4, Nov. 2022. https://doi.org/10.22219/kinetik.v7i4.1551.

[19] T. Janssen, A. Koppert, R. Berkvens, and M. Weyn, "A Survey on IoT Positioning Leveraging LPWAN, GNSS, and LEO-PNT," *IEEE Internet of Things Journal*, vol. 10, no. 13, pp. 11135–11159, 2023. https://doi.org/10.1109/JIOT.2023.3243207.

[20] I. K. A. Enriko, F. N. Gustiyana, and G. C. Giri, "LoRa Gateway Coverage and Capacity Analysis for Supporting Monitoring Passive Infrastructure Fiber Optic in Urban Area," *Elinvo*, vol. 8, no. 2, pp. 164–170, Jan. 2024. https://doi.org/10.21831/elinvo.v8i2.59280.

[21] T. Handoko et al., "Design of GPS Tracker with Long Range (LoRa) Communication to Know the Position of Mountain Climbers," *Telekontran: Jurnal Ilmiah Telekomunikasi, Kendali dan Elektronika Terapan*, vol. 12, no. 2, pp. 162–176, Oct. 2024. https://doi.org/10.34010/telekontran.v12i2.13890.

[22] A. Abdul Wahid, "Waterfall Method Analysis for Information System Development," *Jurnal Ilmu-ilmu Informatika dan Manajemen STMIK*, 2020.

[23] Y. Erdani, R. A. Pratama, B. A. Ahad, and G. I. F. Fadila, "Container Station Control System Design Using the Internet of Things (IoT) Based Waterfall Method," *G-Tech: Jurnal Teknologi Terapan*, vol. 8, no. 3, pp. 1415–1430, Jul. 2024. https://doi.org/10.33379/gtech.v8i3.4315.

[24] N. Zlatanov, "Arduino and Open Source Computer Hardware and Software," 2015. https://doi.org/10.13140/RG.2.1.1071.7849.

[25] K. Sidharta and T. Wibowo, "Study of Resource Efficiency on the Effectiveness of Database Use: A Case Study of SQL Server and MySQL," *Conference on Business, Social Sciences and Innovation Technology*, vol. 1, no. 1, 2020.

[26] M. Haklay and P. Weber, "OpenStreetMap: User-Generated Street Maps," *IEEE Pervasive Computing*, vol. 7, no. 4, 2008. https://doi.org/10.1109/MPRV.2008.80.

[27] LoRa Alliance Technical Committee Regional Parameters Workgroup, *LoRaWAN™ 1.0.3 Regional Parameters*, 2018.

[28] S. Lin, Z. Ying, and K. Zheng, "Design and Implementation of Location and Activity Monitoring System Based on LoRa," 2019. https://doi.org/10.48550/arXiv.1902.01947.

[29] ICAO, *Advanced Surface Movement Guidance and Control Systems (A-SMGCS) Manual*, 2004.